ISSN 1674-1056
http://cpb.iphy.ac.cn
http://iopscience.iop.org/cpb
中国物理 B
Chinese Physics
中国物理 Chinese Physics B

Annealing-enhanced interlayer coupling interaction inGaS/MoS_2 heterojunctions

Xiuqing Meng(孟秀清), Shulin Chen(陈书林), Yunzhang Fang(方允樟), Jianlong Kou(寇建龙)

Citation: Chin. Phys. B . 2019, 28(7): 078101. **doi:** 10.1088/1674-1056/28/7/078101
Journal homepage: http://cpb.iphy.ac.cn; http://iopscience.iop.org/cpb

What follows is a list of articles you may be interested in

Excellent thermal stability and thermoelectric properties of *Pnma*-phase SnSe in middle temperature aerobic environment

Yu Tang(唐语), Decong Li(李德聪), Zhong Chen(陈钟), Shuping Deng(邓书平), Luqi Sun(孙璐琪), Wenting Liu(刘文婷), Lanxian Shen(申兰先), Shukang Deng(邓书康)
Chin. Phys. B . 2018, 27(11): 118105. **doi:** 10.1088/1674-1056/27/11/118105

Influences of annealing on structural and compositional properties of Al_2O_3 thin films grown on 4H-SiC by atomic layer deposition

Li-Xin Tian(田丽欣), Feng Zhang(张峰), Zhan-Wei Shen(申占伟), Guo-Guo Yan(闫果果), Xing-Fang Liu(刘兴昉), Wan-Shun Zhao(赵万顺), Lei Wang(王雷), Guo-Sheng Sun(孙国胜), Yi-Ping Zeng(曾一平)
Chin. Phys. B . 2016, 25(12): 128104. **doi:** 10.1088/1674-1056/25/12/128104

Low specific contact resistivity to graphene achieved by AuGe/Ni/Au and annealing process

Shu-Zhen Yu(于淑珍), Yan Song(宋焱), Jian-Rong Dong(董建荣), Yu-Run Sun(孙玉润), Yong-Ming Zhao(赵勇明), Yang He(何洋)
Chin. Phys. B . 2016, 25(11): 118101. **doi:** 10.1088/1674-1056/25/11/118101

Effects of Fe additive on diamond crystallization from carbonyl nickel powders-C system under HPHT condition

Li Yong, Jia Xiao-Peng, Feng Yun-Guang, Fang Chao, Fan Li-Juan, Li Ya-Dong, Zeng Xiang, Ma Hong-An
Chin. Phys. B . 2015, 24(8): 088104. **doi:** 10.1088/1674-1056/24/8/088104

Annealing effect of platinum-incorporated nanowires created by focused ion/electron-beam-induced deposition

Fang Jing-Yue, Qin Shi-Qiao, Zhang Xue-Ao, Liu Dong-Qing, Chang Sheng-Li
Chin. Phys. B . 2014, 23(8): 088111. **doi:** 10.1088/1674-1056/23/8/088111

Annealing-enhanced interlayer coupling interaction in GaS/MoS_2 heterojunctions*

Xiuqing Meng(孟秀清)†, Shulin Chen(陈书林), Yunzhang Fang(方允樟), and Jianlong Kou(寇建龙)

Zhejiang Provincial Key Laboratory of Solid State Optoelectronic Devices, Zhejiang Normal University, Jinhua 321004, *China*

(Received 11 March 2019; revised manuscript received 12 April 2019; published online 31 May 2019)

Fabrication of large-area atomically thin transition metal dichalcogenides is of critical importance for the preparation of new heterojunction-based devices. In this paper, we report the fabrication and optical investigation of large-scale chemical vapor deposition (CVD)-grown monolayer MoS_2 and exfoliated few-layer GaS heterojunctions. As revealed by photoluminescence (PL) characterization, the as-fabricated heterojunctions demonstrated edge interaction between the two layers. The heterojunction was sensitive to annealing and showed increased interaction upon annealing at 300 °C under vacuum conditions, which led to changes in both the emission peak position and intensity resulting from the strong coupling interaction between the two layers. Low-temperature PL measurements further confirmed the strong coupling interaction. In addition, defect-related GaS luminescence was observed in our few-layer GaS, and the PL mapping provided evidence of edge interaction coupling between the two layers. These findings are interesting and provide the basis for creating new material systems with rich functionalities and novel physical effects.

Keywords: chemical vapor deposition (CVD) growth, two-dimensional (2D) heterojunctions, annealing, strong coupling

PACS: 81.07.–b, 78.55.–m, 78.67.Pt, 68.03.Cd **DOI:** 10.1088/1674-1056/28/7/078101

1. Introduction

Two-dimensional (2D) materials have triggered great research interest since the discovery of graphene, in which quantum coupling exists between the 2D atomic layers stacked through van der Waals forces.[1] These materials have potential applications in optoelectronics, solar cells, transistors, photodetectors, and catalysts.[2–11] In addition, 2D soft matters have great advantages, such as light weight, structural control, flexibility, and diversity of fabrication approaches, and are thus indispensable to the branches of materials science. The fabrication strategies developed so far for 2D nanomaterials mainly involve the exfoliation of layered crystals, chemical vapor deposition (CVD), chemical synthesis, template synthesis, self-assembly, and the combination of some of the above methods.[12,13] Thus, 2D soft nanomaterials are fascinating research subjects from the perspectives of both fundamental study and practical applications.[14]

The softness and flexibility of the layered structures enable us to tailor their optoelectronic properties freely. For example, 2D materials have layer-dependent bandgaps, such as MoS_2, whose indirect bandgap of 1.3 eV in the bulk crossovers to a direct bandgap of 1.9 eV in the monolayer. Moreover, it is desirable to achieve a wider optical spectral response by systematically controlling the bandgap of layered MoS_2, such as by forming heterostructures with other 2D materials. MoS_2-based hybrid materials are very interesting and challenging from a fundamental point of view, and they have only begun to make their way into the broader fields of science and technology from both experimental and theoretical studies.[15–18]

Heterojunction fabrication methods have been shown to exert a profound effect on the properties of MoS_2. For example, MoS_2/WS_2 heterojunctions were fabricated and their gas-dependent low-temperature photoluminescence (PL) was studied.[19] Moreover, WSe_2/MoS_2 photodiodes have been investigated.[20] In addition, 2D GaS has good photoresponse properties and is a promising material for photodetectors.[21] MoS_2/GaS heterojunctions are also a potential candidate for photodetectors. In this regard, we fabricated MoS_2/GaS heterojunctions and studied their optical properties. We found that their interaction coupling increased upon annealing, leading to an enhanced band shoulder emission. Interestingly, we observed defect-related emission of GaS, which is believed to be non-emissive because it is an indirect-bandgap material.

2. Experimental details

GaS was fabricated by the so-called exfoliation method, while MoS_2 was synthesized by the CVD method.

Typically, for MoS_2 growth, MoO_3 (0.3 g, Aladin, 99.9% purity) was placed in an alumina boat in the center of a horizontal quartz tube furnace with one-inch tube diameter. After being cleaned with acetone, isopropyl alcohol, and deionized water, a SiO_2/Si substrate (300 nm thickness) was placed up-

*Project supported by the National Natural Science Foundation of China (Grant Nos. 11104250, 61274099, and 11774313), the Science Technology Department of Zhejiang Province, China (Grant No. 2012C21007), Zhejiang Province Innovation Team, China (Grant No. 2011R50012), and Zhejiang Provincial Natural Science Foundation, China (Grant No. LY17A040003).

†Corresponding author. E-mail: xqmeng@zjnu.cn

© 2019 Chinese Physical Society and IOP Publishing Ltd

side down above the alumina boat. Then, 0.1 g sulfur was put in another alumina boat and placed upstream of the furnace. The furnace was then heated to 810 °C and kept at this temperature for 5 min. During growth, the temperature of the sulfur region was 180 °C. The reaction was continued for 10 min. After the growth was complete, the furnace was quickly cooled down to room temperature.

Then, a poly (methyl methacrylate) (PMMA) based transfer technique was used to transfer MoS_2 from the growth substrate. The substrate was spin-coated with PMMA at 3000 rpm for 30 s and then baked at 150 °C for 20 min, followed by immersion in a 1 M NaOH solution. Once the heterostructure-coated PMMA floated to the solution surface, it was transferred to deionized water and washed. It was then scooped onto the substrate with a GaS layer and dried. The heterojunction was formed by removing PMMA via dipping into an acetone solution.

The heterojunctions were characterized using a Raman/PL spectrometer (Renishaw Inc.) with a 488 nm laser source. PL measurements were taken with a 5 μm^2 laser spot of 10 μW power at a low temperature of 77 K using a homemade vacuum set-up.

3. Results and discussion

During the growth process, triangular pure monolayer MoS_2 crystals were obtained with a size of about 20 μm. The exfoliated GaS was found to be few-layer flakes with a length of about 40 μm. After transition, the two materials partly overlapped, this construction enabled the measurement of optical properties of both the overlapped and non-overlapped parts. We could then easily compare the properties of each material before and after the formation of heterojunctions, as shown in Fig. 1(a).

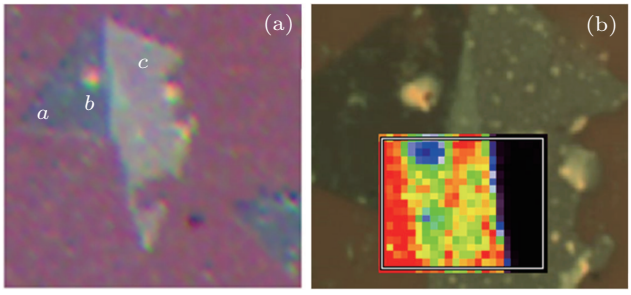


Fig. 1. (a) Microscopic image of the MoS_2/GaS heterojunction, and (b) PL mapping of the heterojunctions.

The PL properties of the as-transferred heterojunctions were studied and their emission spectra are shown in Fig. 2(a). The MoS_2 spectra had dominant exciton peaks at 1.82 eV, which are identical to those observed in the monolayer MoS_2 spectra,[19] this indicates the high optical quality of the materials. Meanwhile, a weak broad emission peak of GaS appeared in the range of 1.8–2.2 eV. It is noteworthy that although GaS is non-emissive because it is an indirect-bandgap material,[22] we observed a weak defect-related GaS emission, which increased after annealing (this will be discussed in the following sections). In the case of heterojunctions, the overlapped part generated a dominant emission peak at 1.84 eV. However, its intensity decreased to some extent, which suggests van der Waals interaction coupling between the two materials. Furthermore, the peak corresponding to the heterojunction blue-shifted by 0.2 eV, indicating the formation of type-II heterojunction between the two materials, wherein both the valence and conduction bands in the core are lower (or higher) than those in the shell, therefore, the energy gradient at the interfaces tends to spatially separate the electrons and holes on different sides of the heterojunction.[23–25] The decrease in peak intensity corresponding to the heterojunction was clearly observed in the PL mapping data (Fig. 1(b)). In Fig. 1(b), the red regions correspond to the strongly luminescent MoS_2, whereas the dark regions correspond to the parts where GaS is located. The mixed region (colored region of the middle part) is consistent with the part of the heterojunction region. After annealing at 300 °C for 1 h in vacuum, evident changes occurred in the heterojunction, and the intensities of peaks corresponding to all parts of the sample increased remarkably.

First, for the bare MoS_2 part, the peak red-shifted from 1.84 eV to 1.829 eV and a broad high-energy shoulder appeared. The high-energy shoulder was believed to originate from nitron-exciton emission of MoS_2, while the dominant peak possibly arose due to a higher density of point defects (S vacancies) and defect clusters created by annealing. As we know, vacancies are a series of highly non-equilibrium, random, and isolated defects, and thermal annealing is much slower and may facilitate the formation of vacancy clusters with different configurations. These defect complexes may have different exciton binding energies, which broaden the observed defect PL peak.[26] Normally, annealing decreases defects at a suitable temperature, however, in our case, annealing not only increased the intensity of emission but also resulted in defect-related emission. This happens because the annealing increased the coupling between the few layer GaS and the atomic layer thick MoS_2. The expanded crystal structure led to an increase in emission intensity, while the coupling between the two materials exerted stress on MoS_2, thereby affecting the structure of MoS_2, resulting in the generation of a MoS_2 shoulder peak. Second, the emission peak of GaS was found at 2.05 eV, which has never been reported before. We believe that this emission peak originated from the defect-related emission of GaS, as it is an indirect-bandgap material. Third, the emission spectrum of the heterojunction, which is the most concerned part, was composed of two dominant peaks, one located at 1.825 eV and the other, a high-energy peak, located

at about 2.05 eV. From the shape of the spectrum, we can deduce that a strong interaction coupling existed between the two parts of the materials, which indicates that annealing enhanced the interaction coupling, as shown in Fig. 2(b).

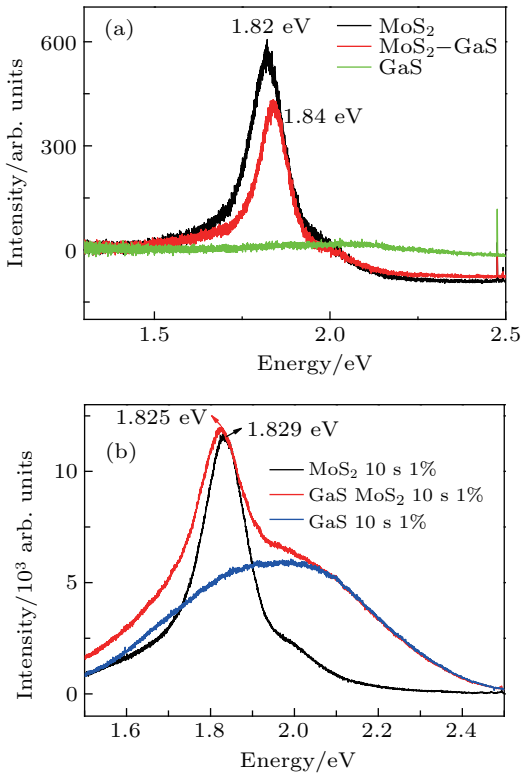


Fig. 2. (a) The PL properties of different parts of the as-transferred heterojunctions. (b) The PL properties of different parts of the 300 °C annealed heterojunctions.

To further study the effect of annealing on the performance of the heterojunctions, power-dependent PL measurements were conducted to study the evolution of emission from the overlapped parts of the heterojunctions, as shown in Fig. 3. The intensity of the emission increased with an increase in excitation power. The non-linear increase in intensity with increasing excitation power indicated that a defect-related emission occurred in the heterojunctions, as seen from the insert in Fig. 3. The defects originated partly from the stress caused by the interlayer coupling and partly from the surface states of MoS_2 and defects of GaS.

Low-temperature PL measurements were carried out to gain further insight into the emission properties of the heterojunction. From the temperature-dependent PL spectra shown in Fig. 4, we found that the intensity of MoS_2 decreased with an increase in temperature, while the peak red-shifted from 1.88 eV at 77 K back to 1.84 eV at 300 K with a decrease in intensity. Moreover, no new peak emerged in the measured range (Fig. 4(a)). In addition, the heterojunction spectrum showed a gradual red shift in the peak position and a decrease in intensity with the increase in temperature (Fig. 4(b)). This phenomenon is similar to that observed for ZnO,[27] and the decrease in intensity is the result of thermal ionization of bound excitons into free excitons at a higher temperature owing to their smaller binding energy.

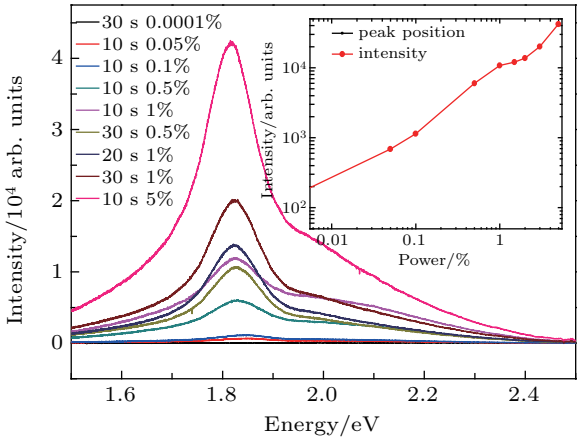


Fig. 3. Power dependent PL of GaS/MoS_2 heterojunctions measured at room temperature, the insert shows the dependence of the PL intensity on the excitation power.

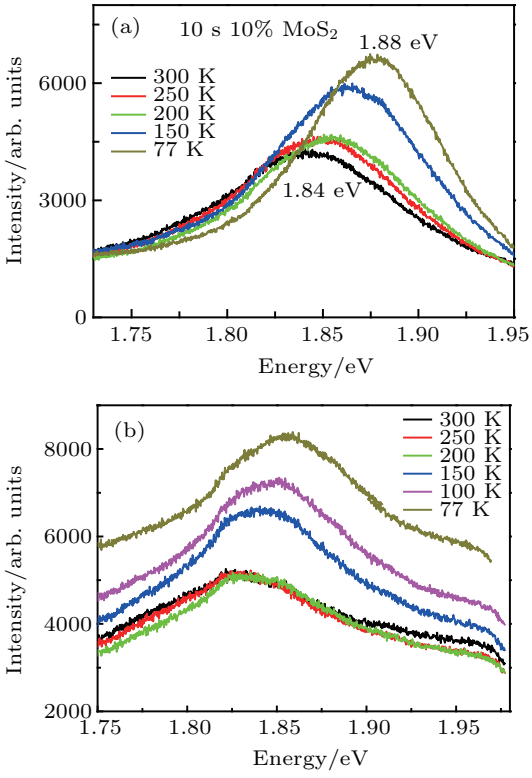


Fig. 4. Temperature dependent PL of (a) MoS_2 and (b) MoS_2/GaS.

4. Conclusion

In summary, we fabricated MoS_2/GaS heterojunctions and studied their optical properties. As seen from the PL study, the as-fabricated heterojunctions demonstrated edge interaction between the two layers and the interaction significantly increased upon annealing at 300 °C under vacuum conditions, which led to changes in both the emission peak position and intensity resulting from the strong coupling inter-

action between the two layers. Low-temperature PL measurements further confirmed the strong coupling interaction. In addition, defect-related GaS luminescence was observed in our few-layer GaS. These findings provide the basis for the study of MoS_2-based heterostructures.

References

[1] Hong X P, Kim J W, Shi S F, Zhang Y, Jin C H, Sun Y H, Tongay S, Wu J Q, Zhang Y F and Wang F 2014 *Nat. Nanotechnol.* **9** 682

[2] Voiry D, Salehi M, Silva R, Fujita T, Chen M W, Asefa T, Shenoy V B, Eda G and Chhowalla M 2013 *Nano Lett.* **13** 6222

[3] Ataca C and Ciraci S 2012 *Phys. Rev. B* **85** 195410

[4] Kibsgaard J, Chen Z, Reinecke B N and Jaramillo T F 2012 *Nat. Mater.* **11** 963

[5] Brivio A J, Giacometti V and Kis A 2011 *Nat. Nanotech.* **6** 147

[6] Radisavljevic B, Whitwick M B and Kis A 2011 *ACS Nano* **5** 9934

[7] Nam H, Wi H, Rokni H, Chen M, Chen M, Priessnitz G, Lu W and Liang X 2013 *ACS Nano* **7** 5870

[8] Zhou G M, Pei S F, Li L, Wang D W, Wang S Y, Huang K, Yin L C, Li F and Cheng H M 2014 *Adv. Mater.* **26** 625

[9] Cao X H, Shi Y M and Shi W H 2013 *Small* **9** 3433

[10] Late D J, Huang Y K and Liu B 2013 *ACS Nano* **7** 4879

[11] Lopez-Sanchez O, Lembke D, Kayci M, Radenovic A and Kis A 2013 *Nat. Nanotech* **8** 497

[12] Chen X, Park Y J and Kang M 2018 *Nat. Commun.* **9** 1690

[13] Zang X N, Chen W S, Zou X L, Hohman J N, Yang L J, Li B X, Wei M S, Zhu C H, Liang J M, Sanghadasa M, Gu J J and Li L W 2018 *Adv. Mater.* **30** 1805188

[14] Tan C, Cao X, Wu X J, He Q, Yang J, Zhang X, Chen J, Zhao W, Han S, Nam G H, Sindoro M, Zhang H 2017 *Chem. Rev.* **117** 6225

[15] Fabrice L, Pierre R, Nico A J M S and Andreas T 2015 *Eur. J. Inorg. Chem.* 1089

[16] Li Q Z, Tang L P, Zhang C X, Wang D, Chen Q J, Feng Y X, Tang L M and Chen K Q 2017 *Appl. Phys. Lett.* **111** 171602

[17] Wu N N, Yang Z X, Zhou W Z, Zou H, Xiong X, Chen Y and Ouyang F P 2015 *J. Appl. Phys.* **118** 084306

[18] Cao N T, Zhang L, Lu L, Xie H P, Huang H, Niu D M and Gao Y L 2014 *Acta Phys. Sin.* **63** 167903 (in Chinese)

[19] Tongay S, Zhou J, Ataca C, Liu J, Kang J S, Tyler S M, Long Y, Li J B, Jeffrey C G and Wu J Q 2013 *Nano Lett.* **13** 2831

[20] Lee H S, Ahn J, Shim W Y, Im S and Hwang D K 2018 *Appl. Phys. Lett.* **113** 163102

[21] Ma Y, Dai Y, Guo M, Yu L and Huang B 2013 *Phys. Chem. Chem. Phys.* **15** 7098

[22] Cai H, Kang J, Sahin H, Chen B, Suslu A, Wu K D, Peeters F, Meng X Q and Tongay S 2016 *Nanotechnology* **27** 065203

[23] Li J and Wang L W 2004 *Chem. Mater.* **16** 4012

[24] Meng X Q, Peng H W, Gai Y Q and Li J B 2010 *J. Phys. Chem. C* **114** 1467

[25] Kumar S, Jones M, Lo S S and Scholes G D 2007 *Small* **3** 1633

[26] Tongay S, Suh J, Ataca C, Fan W, Luce A, Kang J S, Liu J, Ko C Y, Raghunathanan R, Zhou J, Ogletree F, Li J B, Grossman J C and Wu J Q 2013 *Sci. Rep.* **3** 2657

[27] Meng X Q, Shen D Z, Zhang J Y, Zhao D X, Dong L, Lu Y M, Liu Y C and Fan X W 2005 *Nanotechnology* **16** 609